CHAPTER - 3

ESTIMATION OF SOIL MOISTURE BY GROUND BASED BISTATIC SCATTEROMETER DATA AT X-BAND

CHAPTER-3

ESTIMATION OF SOIL MOISTURE BY GROUND BASED BISTATIC SCATTEROMETER DATA AT X-BAND

3.1 INTRODUCTION

Soil moisture is an important variable for hydro-meteorological applications (Ahmad et al. 2010) and has significant effect on catchment water balance, water yield, groundwater recharge, and storage (Al-Shrafany et al. 2012; Srivastava et al. 2013c; Zhang et al. 2001). The study of spatial and temporal soil moisture distribution on the top ground surfaces is very necessary at regional as well as on global scale (Srivastava et al. 2013a). Furthermore, consistent estimates of soil moisture from cropped surfaces are required for efficient irrigation management and scheduling (Glenn et al. 2011; Lorite et al. 2012). *In-situ* observations of soil moisture such as those from probe or gravimetric measurements are available and could be used for soil moisture, but they do not represent the spatial distribution accurately as soil moisture is highly variable both spatially and temporally and hence unsuitable for large scale applications (Srivastava 2013; Srivastava et al. 2013b; Wang and Qu 2009). On the other hand satellite remote sensing is found suitable for soil moisture retrieval with high accuracy (Kerr et al. 2012).

Microwave remote sensing is a powerful tool to monitor the soil moisture over the soil surfaces (Srivastava et al. 2014). Nowadays, it is becoming much popular than the optical sensors due to its adequate capability to acquire observations in all weather conditions and all the time (day and night) (Owe et al. 2001a). In context of soil moisture, several researchers (Chauhan 1997; Engman and Chauhan 1995; Njoku and Li 1999; Schmugge et al. 1986; Ulaby et al. 1981; Wang et al. 1983) have conducted experiments using monostatic radar geometry (ground based, airborne and space borne) to develop empirical, semi empirical and theoretical models for the estimation of soil surface parameters by active and passive microwave remote sensing. However, only limited number of bistatic experiments have been conducted (Khadhra et al. 2012; Singh et al. 1996) and reported in the technical literature domain. Thus, this study is important for microwave remote sensing community to understand the interaction of X- band bistatic radar with soil moisture and its performances towards

soil moisture retrieval. The space mission has been started by German Space Agency, with twins satellite (TanDEM-X and TerraSAR-X) for bistatic radar to generate a three dimensional image of the earth.

It is very difficult to understand the scattering mechanism of microwave with the natural soil surfaces. During the last decade, many useful modeling approaches based on linear regression analysis and non parametric algorithms like artificial neural network (ANN), support vector regression (SVR), fuzzy logic (FL) etc have been reported for the estimation of soil moisture and soil surface parameters (Oh et al. 1992; Saleh et al. 2006; Singh 2005; Singh et al. 1996). These models have advantages to provide reasonable results in most of the cases. For e.g. the linear regression models based on least square method is widely used for establishing the linear relation between the scattering coefficients and soil moisture content. The ANN is a model free estimator and it acquires a highly non-linear input-output relationship through a process called training. Several researchers (Chai et al. 2009; Del Frate et al. 2003; Dharanibai and Alex 2009; Jiang and Cotton 2004) have widely used ANN for the estimation of surface soil moisture. However, rare studies have been reported using the bistatic scatterometer data for the retrieval of soil moisture.

In purview of the above, the foremost objective of this chapter is to acquire the suitable and reliable model for the estimation of soil moisture using microwave bistatic scatterometer data at X-band. The performances of several models such as BPANN, RBFANN and GRANN and the LRM are attempted in this study to estimate the soil moisture. The remainder of this chapter is structured as follows: In section 2, we introduce the experimental procedure, which provides a brief overview of the instrumentation and field measurements. In section 3, the description of selected techniques are provided and the criteria for the assessment is listed. In section 4, the results obtained from all the approaches are presented and discussed. The last section 5 contains the conclusions, which provides the final remark and conclusion of this work.

3.2 EXPERIMENTAL DETAILS

The specifications of bistatic scatterometer set-up employed for the outdoor bistatic measurements at different moisture content of slightly rough bare soil surface is shown in Table 2.1 and the detailed procedure for the bistatic scatterometer measurements is given in the Chapter 2.

All the observations were carried out by changing the incidence (θ_i) and receiving angles (θ_r) in the angular range of 20° to 70° at steps of 5° in the elevation direction for azimuthal angle (ϕ= 0). The incident wave gets scattered in all the directions due to the soil surface roughness and moisture content. The scattered wave may be presented in terms of diffuse and coherent components. Most probably, the coherent component of the scattered wave has been received in the specular direction. It means, the highest power reflecting from the slightly rough bare soil surface has been observed in the present study.

Figure 3.1 shows the surface roughness profile, autocorrelation function and the comparison of soil surface autocorrelation function with the Gaussian and exponential autocorrelation functions. The surface roughness was taken constant during entire observations to study the microwave response of soil moisture content only. The root mean square height (σ) and correlation length (l) of the test soil surface were 1.61 cm and 11.63 cm respectively.

3.3 DESCRIPTION OF DIFFERENT KIND OF ARTIFICIAL NEURAL NETWORK MODELS

In the present study, three different ANN algorithms were used for the retrieval of soil moisture using bistatic scatterometer data. ANN algorithms are easy to perform the non-linear complex statistical modeling between dependent and independent variables. One of the advantages of ANN is its non-parametric nature whereas most of the statistical models are parametric in behavior. In the ANN, the optimum value of free parameters are adjusted by training of the ANN algorithms using large input-output data sets while most of statistical methods are parametric model that need higher background of statistic. The ANN algorithms have ability to implicitly detect complex nonlinear relationships between dependent and independent variables by

training. Disadvantages include greater computational burden, proneness to over fitting, and the empirical nature of model development.

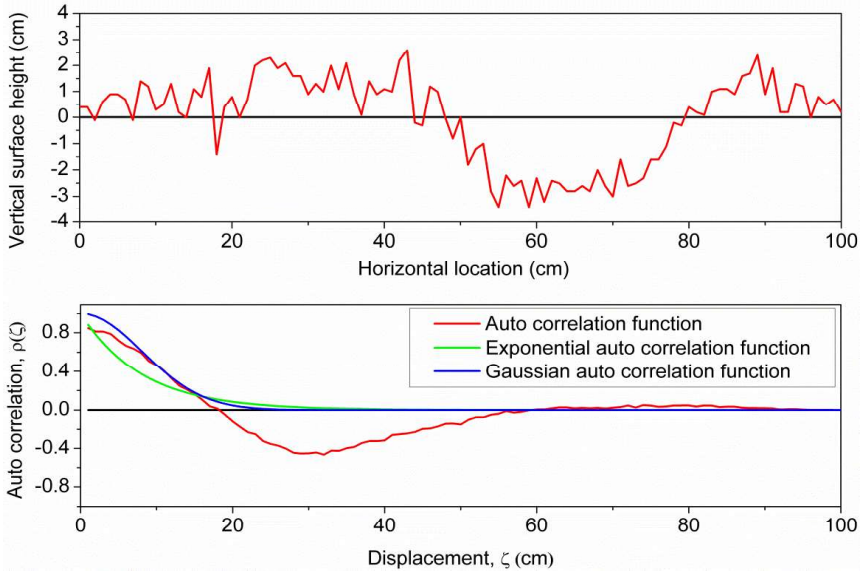

Figure 3.1 Surface roughness profile and auto correlation function for test soil surface (RMS height (σ) = 1.61cm and correlation length (l) = 11.69 cm)

3.3.1 BACK PROPAGATION ARTIFICIAL NEURAL NETWORK (BPANN)

In BPANN, the simple processing units (neuron) are arranged in different layers as input, hidden and output layers. The inputs are applied at input layer of ANN. The input layer propagates information in the forward direction to each node of the hidden layer with their synaptic weights. At each node, these weighted inputs are added. Each hidden layer computes output corresponding to these weighted sums through linear/non-linear sigmoidal transfer functions (Erbek et al. 2004; Haykin 1994, 1999a). Figure 3.2 shows the specific structure of BPANN used in the present study.

The output values computed from each hidden layer nodes become input values for nodes of the output layer. These inputs for output layer nodes are obtained with the weighted sum and processed through transfer function at the output layer. Such nodes of output layer compute the final output of BPANN corresponding to their inputs. These computed output values are compared with the desired output values. Therefore, corresponding error is estimated at the output layer between computed

output values and desired output values. The estimated errors are sent back to the ANN. The connection weights and biases are modified accordingly until desired results are achieved. This process is repeated iteratively and connection weights and biases are modified until the convergence reached to an acceptable error. Therefore, the estimated values by BPANN may be very close to the observed values.

3.3.2 RADIAL BASIS FUNCTION ARTIFICIAL NEURAL NETWORK (RBFANN)

RBFANN model is based on the function approximation and data interpolation. The RBFANN consists of three different feed forward layers namely input layer, hidden layer and output layer. The hidden layer neurons are implemented with radial basis functions (e.g. Gaussian function). The output layer neurons are implemented with linear summation functions as in a multilayer perceptron. The Gaussian function is defined as,

$$\Phi(r) = exp\left(-\frac{(x-c)^2}{2\sigma^2}\right) \tag{3.1}$$

where σ and c are the spread factor and center respectively. All the hidden layer neurons take inputs from all input layer neurons. The hidden layer neurons are activated with radial basis function having center and spread parameters. The selective function decreases rapidly with smaller value of spread whereas it decreases slowly with the larger value of spread.

The center of the radial basis function for i^{th} neuron at the hidden layer is a vector c_i whose size is as the input vector x. The radial distance d_i, between the input vector x and center of the radial basis function c_i are computed for each i^{th} neurons in the hidden layer as,

$$d_i = \|x - c_i\|, \quad i = 1, 2, 3, \ldots\ldots\ldots\ldots h. \tag{3.2}$$

Using the Euclidean distance, the output for each i^{th} neurons of the hidden layer were computed by applying the radial basis function $\phi(r)$ to the Euclidean distance,

$$H_i = \emptyset(d_i, \sigma_i) \tag{3.3}$$

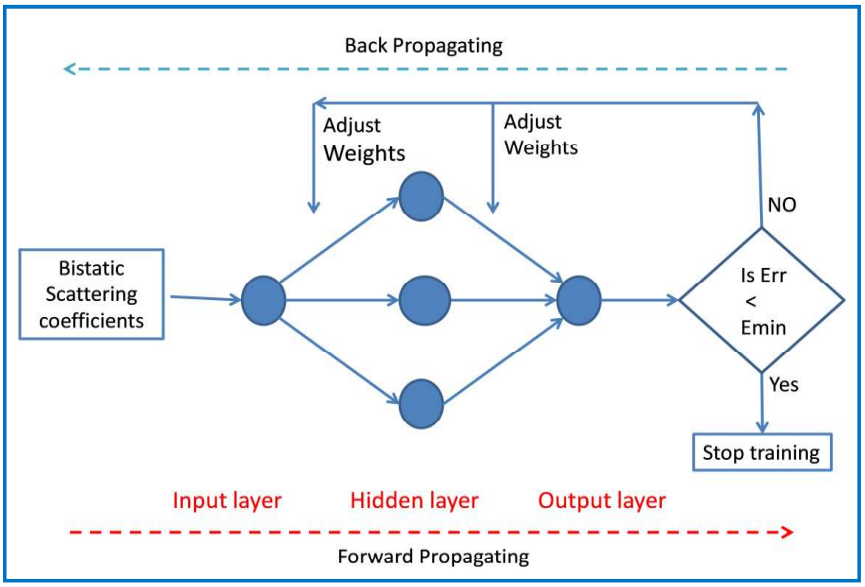

Figure 3.2 Structure of BPANN used in the present study

The calculation made between the input spaces to hidden space is nonlinear whereas the hidden space to output space is linear.

The j^{th} output is computed as,

$$y_j = f_j(\boldsymbol{x}) = w_{oj} + \sum_{i=1}^{h} w_{ij} H_i \qquad (3.4)$$

where

j= 1, 2, 3,……..,m,

y_j= output of j^{th} neuron.

w_{ij} = weight vector for j^{th} neuron.

H_i = output from i^{th} hidden layer neuron.

The value of centre and spread depend on the pattern to be used for optimization. Generally, the spread value should be larger than the minimum distance and smaller than the maximum distance between the input neurons and the centre of the RBFANN spread in order to get better generalization(Narendra et al. 1998). The

centre and weights were found by using the orthogonal least squares (OLS) algorithm (Chen et al. 1991b). Figure 3.3 shows the specific structure and process of RBFANN.

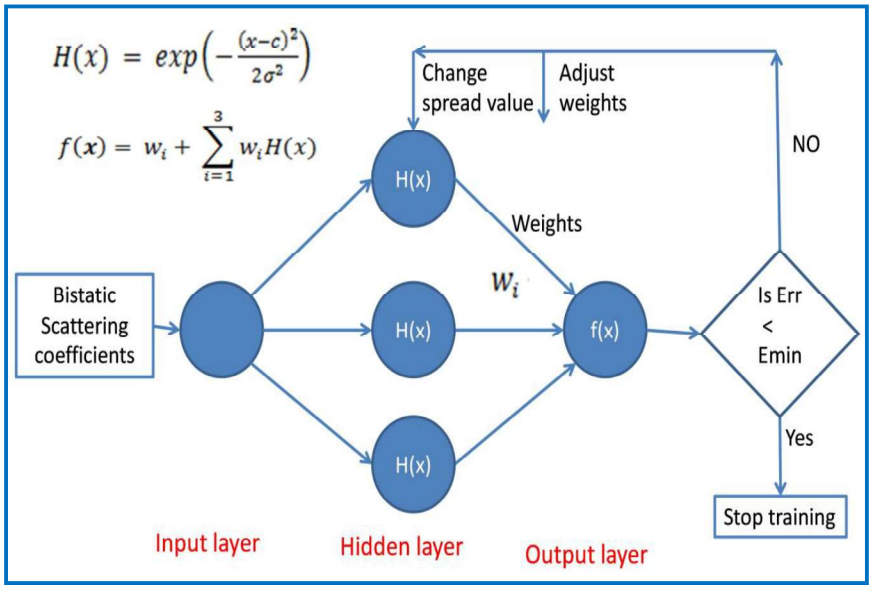

Figure 3.3 Structure of RBFANN model used in the present study

3.3.3 GENERAL REGRESSION ARTIFICIAL NEURAL NETWORK (GRANN)

The GRANN computes the most probable value of an output y for a given training vector x. Specifically, the network computes the joint probability density function for x and y. The expected value of the output y for the input vector x is,

$$E\left[\frac{y}{x}\right] = \frac{\int_{-\infty}^{\infty} y f(x,y)dy}{\int_{-\infty}^{\infty} f(x,y)dy} \tag{3.5}$$

The density function $f(x,y)$ is estimated from the sample of observations made for x and y. The probability estimator

$$\hat{f}(x,y) = \frac{1}{(2\pi)^{\frac{p+1}{2}}\sigma^{(p+1)}} \cdot \frac{1}{n}\sum_{i=1}^{n} \exp\left(-\frac{(x-x^i)^T(x-x^i)}{2\sigma^2}\right) \cdot \exp\left(-\frac{(y-y^i)^2}{2\sigma^2}\right) \tag{3.6}$$

where n and p are the number of sample observations and the dimension of vector x respectively. A physical interpretation of the probability estimate $\hat{f}(x, y)$ is that it assigns sample probability of width σ (smoothing factor or 'width') for each sample x^i and y^i. The probability estimate is the sum of those sample probabilities.

The squared of distance between the input vector x and the training vector x^i is defined as:

$$D_i^2 = \left(x - x^i\right)^T \left(x - x^i\right) \tag{3.7}$$

The final output is determined by,

$$\hat{f} = \frac{\sum_{i=1}^{n} y^i \exp\left(-\frac{D_i^2}{2\sigma^2}\right)}{\sum_{i=1}^{n} \exp\left(-\frac{D_i^2}{2\sigma^2}\right)} \tag{3.8}$$

The smoothing factor (σ) is a very important parameter of GRANN. The estimated density is smooth for large σ, whereas, it is non-smooth for smaller value of σ. Figure 3.4 shows the specific structure of GRANN model.

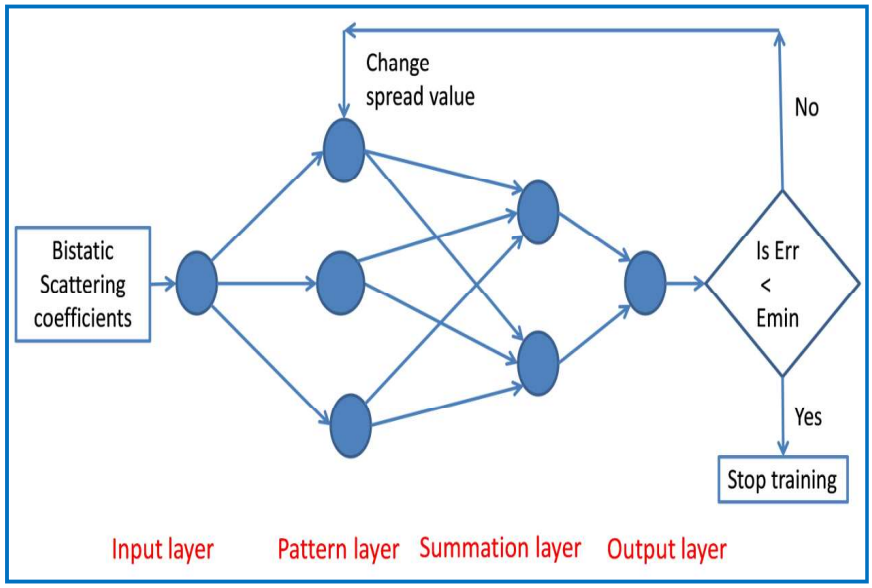

Figure 3.4 Structure of GRANN model used in the present study

3.3.4 LINEAR REGRESSION MODEL (LRM)

The linear regression model establishes the linear relationship by fitting linear equation between the two variables. The first and second variable can be considered as explanatory variable (x_i) and dependent variable (y_i) respectively. This model can be represented by the following equation.

$$y_i = ax_i + b \tag{3.9}$$

where $i = 1, \ldots\ldots\ldots\ldots\ldots, n$. $\boldsymbol{a}$ and $\boldsymbol{b}$ are the slope and intercept respectively. The coefficients (slope and intercept) are computed by the least square method.

3.4 PERFORMANCE INDICES

Several performances indices such as %bias, Root Mean Squared Error (RMSE) and Nash-Sutcliffe Efficiency (NSE) are used for estimating the performances of different models. The percentage bias (%bias) measures the average tendency of the estimated values to be larger or smaller than their observed values. The optimum value of %bias is 0.0 and the smaller value of %bias indicates that accurate model prediction.

$$\%bias = 100 * \left[\frac{\sum(y_i - x_i)}{\sum x_i}\right] \tag{3.10}$$

where x_i is the observed and y_i is the estimated variable.

Root-mean-square error (RMSE) is frequently used to measure the differences between estimated values by a model or an estimator and the observed values.

$$RMSE = \sqrt{\frac{1}{n}\sum_{i=1}^{n}(y_i - x_i)^2} \tag{3.11}$$

where n is the number of observations.

The Nash-Sutcliffe Efficiency (NSE) is based on the sum of absolute of squared of differences between the estimated and observed values normalized by the variance of the observed values. The NSE was calculated using equation (3.12)

$$NSE = 1 - \frac{\sum_{i=1}^{n}(y_i - x_i)^2}{\sum_{i=1}^{n}(x_i - \bar{x}_i)^2} \quad (3.12)$$

3.5 RESULTS AND DISCUSSION

3.5.1 MICROWAVE RESPONSE OF SOIL MOISTURE IN SPECULAR DIRECTION AT X- BAND

Figure 3.5 (a-b) shows the angular variation of bistatic scattering coefficient for slightly rough bare soil surface at various gravimetric soil moisture conditions (11.70%, 15.61%, 20.43% and 24.12%) at HH- and VV-polarization. The soil surface roughness was maintained constant during the entire observations for studying the specular reflection/scattering from the slightly rough bare soil surface at different soil moisture conditions. The bistatic scattering coefficient was found to increase with the percentage of soil moisture content at HH- and VV- polarizations. Several researchers have found similar results (Bertuzzi et al. 1992; Dobson and Ulaby 1981; Khadhra et al. 2012; Ulaby et al. 1982) at X-, C- and L-band. The bistatic scattering coefficient was found to decrease with the incidence angle at VV- polarization and increases at HH-polarization. The scattering from slightly rough bare soil surface depends on the electrical property (dielectric constant), geometrical property (surface roughness) and chemical composition property (soil texture) as well as on the system properties like frequency, polarization and incidence angle.

The surface roughness is one of the important factors for influencing the scattering behaviour of electromagnetic wave from the surface. It is not an intrinsic property; it depends on the wavelength of the transmitted signal with respect to surface roughness. As the wavelength increases, the effect of roughness decreases. The magnitude of surface roughness also depends on the angle of incidence of the transmitted wave. The relation between the surface roughness and EM wave is defined in terms of the statistical property of surface roughness such as ks and kl, where k is the wave number of the transmitted wave defined as $k = \frac{2\pi}{\lambda}$. As the correlation length increases, the surface roughness decreases.

In this study, the RMS height of the bare soil surface was high; however, the high correlation length of the soil surface compensates the surface roughness indicated by the small value of slop (m = 0.19) of the facet in the soil surface. The

bare soil surface under study behaves like a slightly rough surface at 10 GHz. The EM wave interacting with this slightly rough soil surface may be presented in terms of diffuse and coherent components.

The bistatic scatterometer experiment was conducted by changing the incidence angle of the receiving and transmitting antenna at azimuthal angle ϕ=0 in the specular direction. The coherent component of the scattered waves was found to be dominating because of having high gain of receiving and transmitting antennas and their low 3 dB beam widths. The footprint of antenna beam covered the areas of the soil surface under study between 0.2247 m^2 to 2.755 m^2 in the angular range of incidence angle 20° to 70°. The dynamic ranges of angular variation of bistatic scattering coefficient with the various soil moisture contents were found to be 6.79 dB and 10.68 dB at HH- and VV- polarization respectively. At most care was taken to coincide the geometry of receiving and transmitting antenna beam with each other at the same place on the target during the bistatic scatterometer measurements.

According to Fresnel reflection theory for the slightly rough surface, the reflectivity in specular direction was found to increase with the incidence angle at HH-polarization. However, it was found to decrease until the Brewster angle was reached and then after increased slightly in the case of VV-polarization.

3.5.2 EVALUATION OF DATA

Table 3.1 shows the linear regression results between the bistatic scattering coefficient and soil moisture content in the angular range of incidence angle 20° to 70° at steps of 5° for HH- and VV- polarization. These results may be used for the evaluation of data and the selection of suitable incidence angle for the estimation of soil moisture at HH- and VV- polarization. The values of coefficient of determination (R^2) were found higher at lower incidence angles than at higher incidence angles. It means that the bistatic scattering coefficients were more sensitive to the soil moisture content at lower incidence angles than the higher incidence angles. The higher values of (R^2) were found to be 0.868 and 0.886 at 25^0 incidence angle for HH- and VV-polarization respectively. The bistatic scattering coefficients at 25° incidence angle were taken for the estimation of soil moisture by nonparametric models (BPANN, RBFANN and GRANN) and linear regression model (LRM).The data sets at 25°

incidence angle were interpolated to generate 68 data sets for the estimation of soil moisture using artificial neural networks. These 68 data sets were classified in to 17 different groups of data sets. Thus, each such group contains 04 data sets. Out of these 04 data sets, 03 data sets were chosen for training and 01 data set was taken for validation of ANN models from all the 17 different groups of data set.

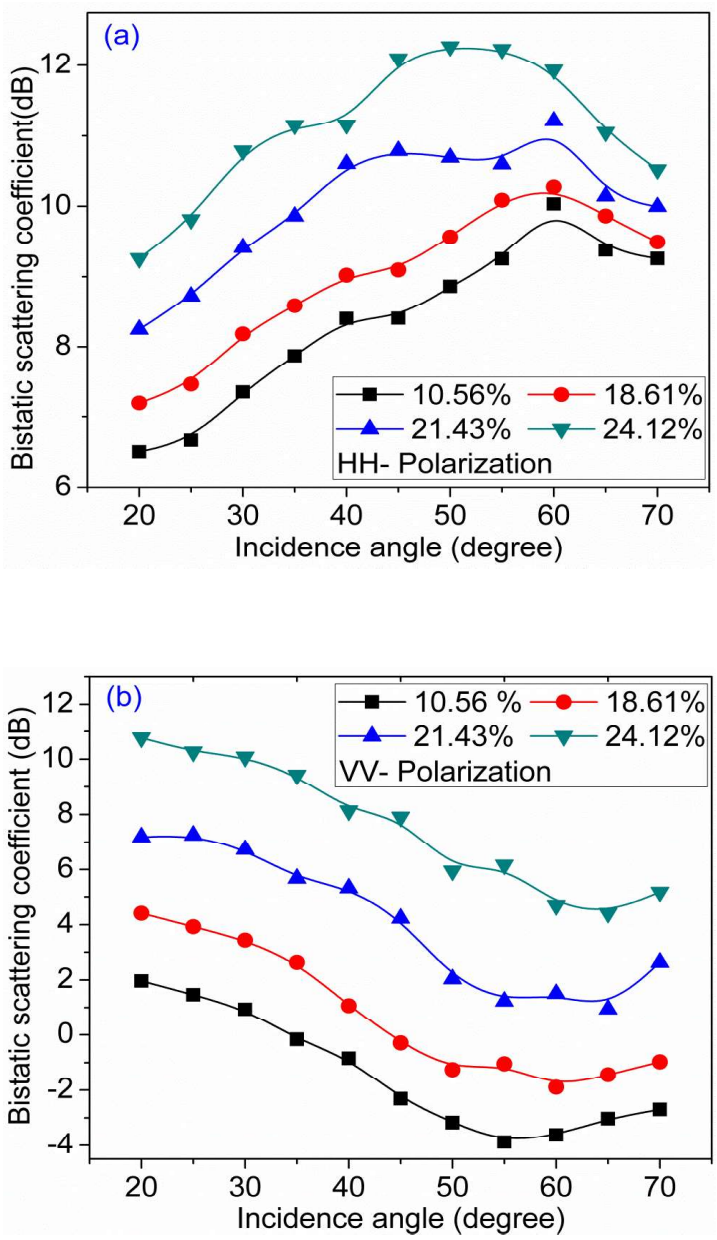

Figure 3.5 Angular variation of scattering coefficients at various soil moisture contents for (a) HH- and (b) VV- polarization at X-band

Table 3.1 Linear regression results between bistatic scattering coefficient and soil moisture

Angle (°)	HH- Pol.			VV- Pol.		
	R^2	SE	SEE	R^2	SE	SEE
20	0.864	0.561	0.386	0.872	1.765	1.174
25	0.868	0.645	0.436	0.886	1.810	1.125
30	0.851	0.691	0.501	0.878	1.863	1.201
35	0.837	0.662	0.506	0.883	1.935	1.219
40	0.846	0.597	0.440	0.844	1.868	1.392
45	0.821	0.755	0.609	0.829	2.088	1.644
50	0.809	0.668	0.563	0.823	1.814	1.460
55	0.808	0.564	0.476	0.840	1.947	1.470
60	0.775	0.386	0.360	0.831	1.684	1.313
65	0.816	0.318	0.262	0.812	1.459	1.216
70	0.810	0.253	0.212	0.847	1.631	1.199

3.5.3 ESTIMATION OF SOIL MOISTURE USING THREE DIFFERENT ARTIFICIAL NEURAL NETWORK ARCHITECTURES AND LINEAR REGRESSION MODEL

Three different ANN architectures (BPANN, RBFNN and GRANN) and linear regression model (LRM) were used for the estimation of soil moisture content from the slightly rough soil surfaces in the angular ranges of 20° to 70° at HH- and VV- polarization using X-band bistatic scatterometer data. The observed data sets (bistatic scattering coefficient and soil moisture content) were interpolated into 68 data sets at the incidence angle 25° for HH- and VV- polarization. The procedure for the selection of training and validation data sets is given in Section 3.5.2.

Table 3.2 shows the optimum parameters of BPANN, RBFANN and GRANN models for HH and VV polarization. The parameters of ANN techniques need to be optimized for the accurate result. The preliminary analysis of ANN techniques is necessary before using it for any estimation. This study began with three ANN techniques namely BPANN, RBFANN and GRANN. In the BPANN, number of hidden layers, transfer function for each hidden layer and output layer, number of neurons in each layer, momentum, training algorithm, learning rate, number of iterations and size of training data sets are very important parameters for getting the

desired result. The optimization of these parameters are very challenging task. During the training of the ANN, the performance of ANN model is checked at different configurations using trial-error method. In trial-error method, the efforts were made to minimum value of RMSE between estimated and observed soil moisture content for each spread value.

The number of iterations also plays a major role during the training of BPANN. The BPANN results may vary according to the number of iterations even for the same parameters during the training of networks. Thus, it is needed to retrain the network 3 or 4 times using the same parameters to select the optimum number of iterations. The number of neurons at input and output layer of BPANN may be equal to the number of input-output parameters in the data sets. The number of neurons at hidden layer may vary for the optimization of BPANN to achieve accurate retrieval of soil moisture content.

The value of spread is an important parameter to optimize the RBFANN and GRANN models for the training. Generally, the spread value should be larger than the minimum distance and smaller than the maximum distance between the input neurons and the centre of the RBFANN in order to get better optimization. The optimum value of spread is found by training the models using spread values between 1 and 15 at steps of 0.5 by trial-error method. In the above range of spread values, the values of RMSE shown by the RBFANN and GRANN models are found either constant or slightly higher RMSE with the increase of spread values at HH polarization. The relationship established between bistatic scattering coefficients and soil moisture content may not be fruitful by using higher value of spread at HH polarization. Moreover, many neurons may be required to fit the rapidly-changing function in the case of taking either larger or smaller spread value. The higher number of neurons may reduce the optimization speed of the model. On the basis of the above analysis, the performance of RBFANN and GRANN models is found optimized at the spread value 1 for HH polarization.

In case of VV polarization, the RBFANN model gives the lowest values of RMSE up to spread value 3 and then its value was higher but found constant in the range of 4 to 15 spread value. Thus, the spread value was chosen 1 for the RBFANN

model. However, the GRANN model gave the constant RMSE in the entire range of spread values between 1 and 15. Thus, the spread value for the GRANN model was chosen 1 at VV polarization.

The performance during the training and validation of different ANN models and linear regression model for the estimation of soil moisture were evaluated in terms of %bias, root mean square error (RMSE) and Nash-Sutcliffe Efficiency (NSE). Table 3.3 and 3.4 depict the performance indices during training and validation for the estimation of soil moisture by BPANN, RBFANN, GRANN and LRM respectively.

Figure 3.6 (a-b) and Figure 3.7 (a-b) depict the scatter plots between experimentally observed and estimated soil moisture by all the four models during the training and validation of models respectively. On the basis of computed performance indices like %bais, RMSE and NSE, the performance of BPANN and GRANN models were found better than the other models at HH- and VV- polarization respectively for the estimation of soil moisture during the training of the models. During the validation of models, the performance of BPANN and RBFANN models were found better than the other models at HH and VV polarization respectively for the estimation of soil moisture. Among different models, the BPANN is found to have marginally higher performance in case of HH polarization while RBFANN is found suitable with VV polarization followed by GRANN and LRM. The RBFANN model was found better estimator among the three estimators (BPANN, GRANN and LRM) for the estimation of soil moisture of bare soil surfaces at VV polarization. The performance of models for the estimation of soil moisture is evaluated by comparing the values of performance indices summarized in Tables 3.3 and 3.4.

The performance of LRM model is compared with all the three ANN models on the basis of their corresponding NSE and RMSE. During the training of the models, the difference of the performance indices (NSE and RMSE) corresponding to BPANN and LRM models are found 0.0556 and 0.03449 respectively at HH-polarization. Whereas, the difference between the performance indices corresponding to GRANN and LRM models are found 0.0333 and 0.2067 for NSE and RMSE respectively at VV- polarization. During the validation of the models, the difference between the performance indices corresponding to BPANN and LRM models are

found 0.0312 and 0.2142 for NSE and RMSE respectively at HH polarization. At VV polarization, the difference between performance indices corresponding to RBFANN and LRM model are found 0.0293 and 0.2140 for NSE and RMSE respectively.

The above analysis shows small differences of NSE and RMSE corresponding to ANN and LRM models. This indicates almost similar performances of ANN in comparison to the LRM model. Thus, the LRM model may be the better approach for the estimation of soil moisture content of slightly rough surface using bistatic scatterometer data. The LRM is seemed to be the simple in operation than the ANN models for the estimation of soil moisture. Figure 3.8 shows the flow chart for comparing the results obtained by the different ANN models and LRM models.

Table 3.2 Optimization of ANN model parameters

	HH-Polarization			VV-Polarization		
Optimum parameters	BPANN	RBFANN	GRNN	BPANN	RBFANN	GRANN
Number of hidden layers	1	1	-	1	1	-
Number of neurons at hidden layer	3	3	-	3	3	-
Number of neurons at output layer	1	-	-	1	-	-
Number of neurons at pattern layer			3			3
Transfer function at hidden layer	Hyperbolic tangent sigmoidal	Gaussian function	-	Hyperbolic tangent sigmoidal	Gaussian function	-
Transfer function at output layer	Linear	Linear	-	Linear	Linear	-
Training algorithms	Gradient descent	-	-	Gradient descent	-	-
Momentum	0.9	-	-	0.9	-	-
Learning rate	0.1	-	-	0.1	-	-
Spread	-	1	1	-	1	1

Table 3.3 Performance indices during training

Models	HH- Polarization			VV- Polarization		
	%Bias	RMSE	NSE	%Bias	RMSE	NSE
BPANN	9.03E-05	1.0981	0.9216	-0.3643596	1.2572	0.8973
RBFANN	3.62E-04	1.2728	0.8947	1.03E-05	1.1446	0.9148
GRANN	-0.9265517	1.6908	0.8142	-0.2223330	1.138	0.9158
LRM	-2.29E-06	1.443	0.8647	1.14E-06	1.3447	0.8825

Table 3.4 Performance indices during validation

Models	HH- Polarization			VV- Polarization		
	%Bias	RMSE	NSE	%Bias	RMSE	NSE
BPANN	-0.1243166	1.01	0.9336	-0.8117412	0.9732	0.9383
RBFANN	-0.7344098	1.0628	0.9265	-0.8246147	0.9389	0.9426
GRANN	-1.9434577	1.5369	0.8462	-0.8745645	0.9777	0.9378
LRM	-0.6289193	1.2242	0.9024	-0.5367848	1.1539	0.9133

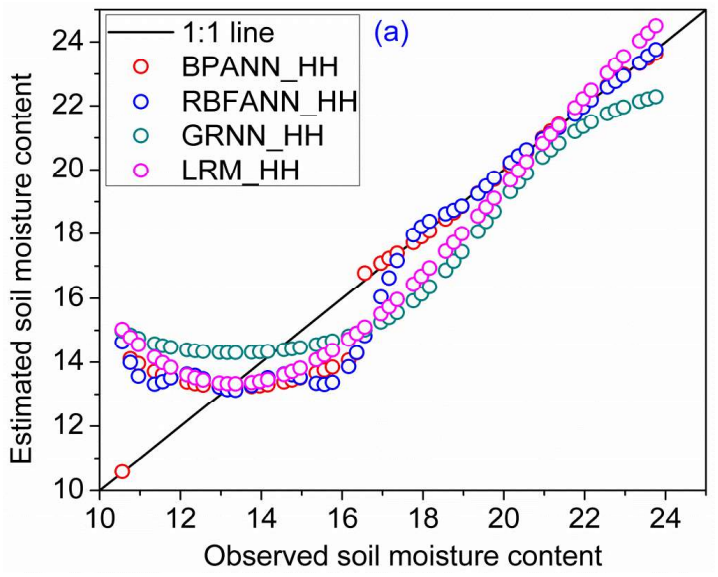

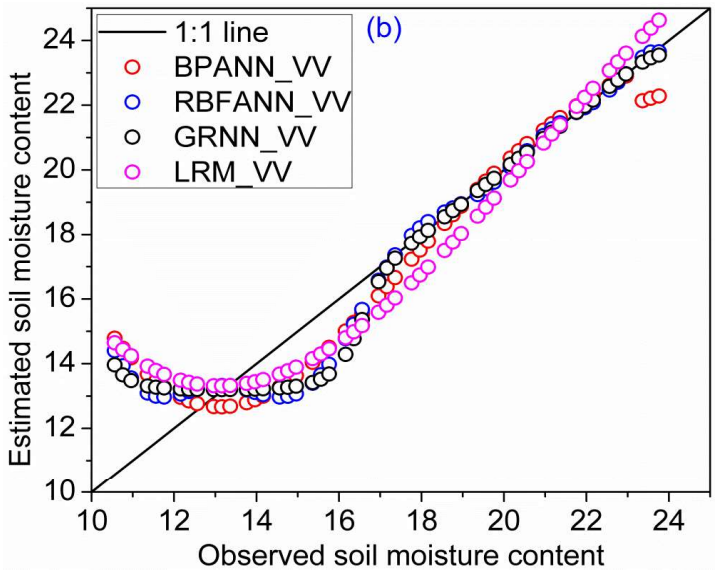

Figure 3.6 Scatter plot between observed and estimated soil moisture for the training of models at (a) HH- polarization and (b) VV- polarization with 1:1 lines

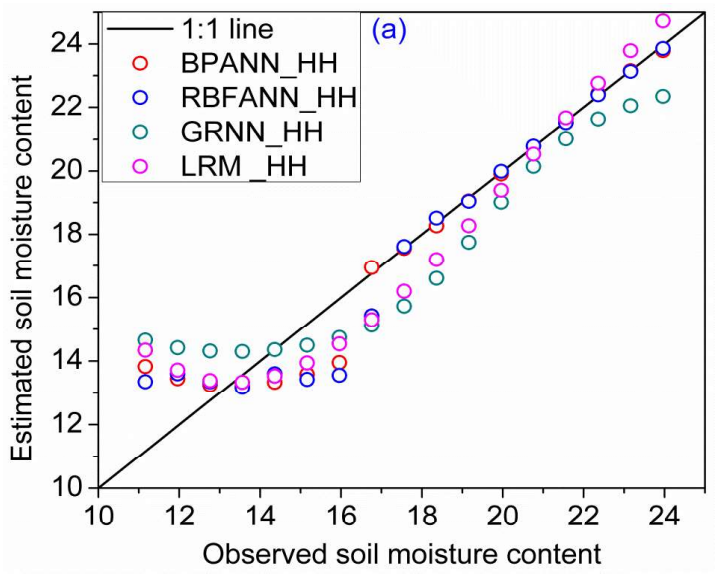

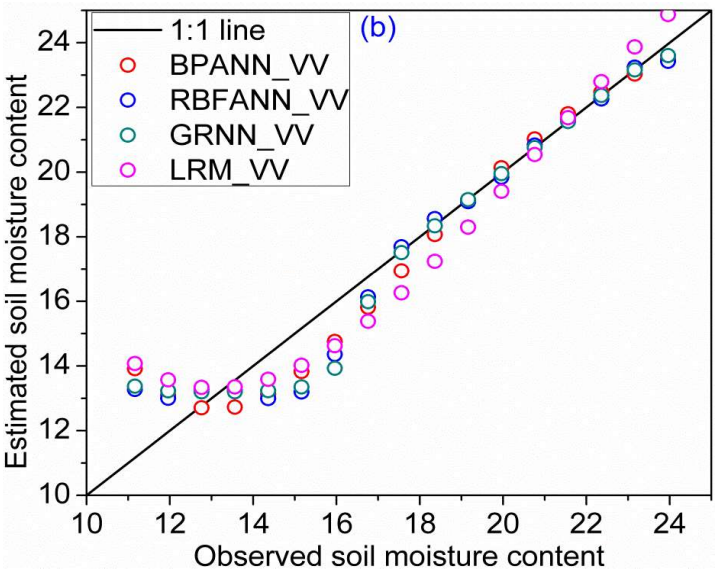

Figure 3.7 Scatter plot between observed and estimated soil moisture for the validation of models at (a) HH- polarization and (b) VV- polarization with 1:1 lines

In Figures 3.9 and 3.10, the Taylor plots were used to compare the quality of performance of the different non parametric or parametric models for the estimation of soil moisture by bistatic scatterometer data during the training and validation respectively. The circle mark along the X-axis on the Taylor plot is called as the reference point using observed data. The color points on the Taylor plot were drawn using estimated data by different models used in study. The colored point on the Taylor closer to circle point represents the perfect fit between observed and estimated data by the different approaches made in the present study. It also indicates the tendency of over/under estimation of data. If the standard deviation of the estimated values is found higher than the standard deviation of observed values, then it will result into overestimation and vice-versa. Taylor plot also indicates high correlation between observed and estimated values of soil moisture content during training and validation of all the models (parametric or non-parametric). However, the GRANN model provided lower efficiency for the estimation of soil moisture during training and validation than the other models at HH- polarization.

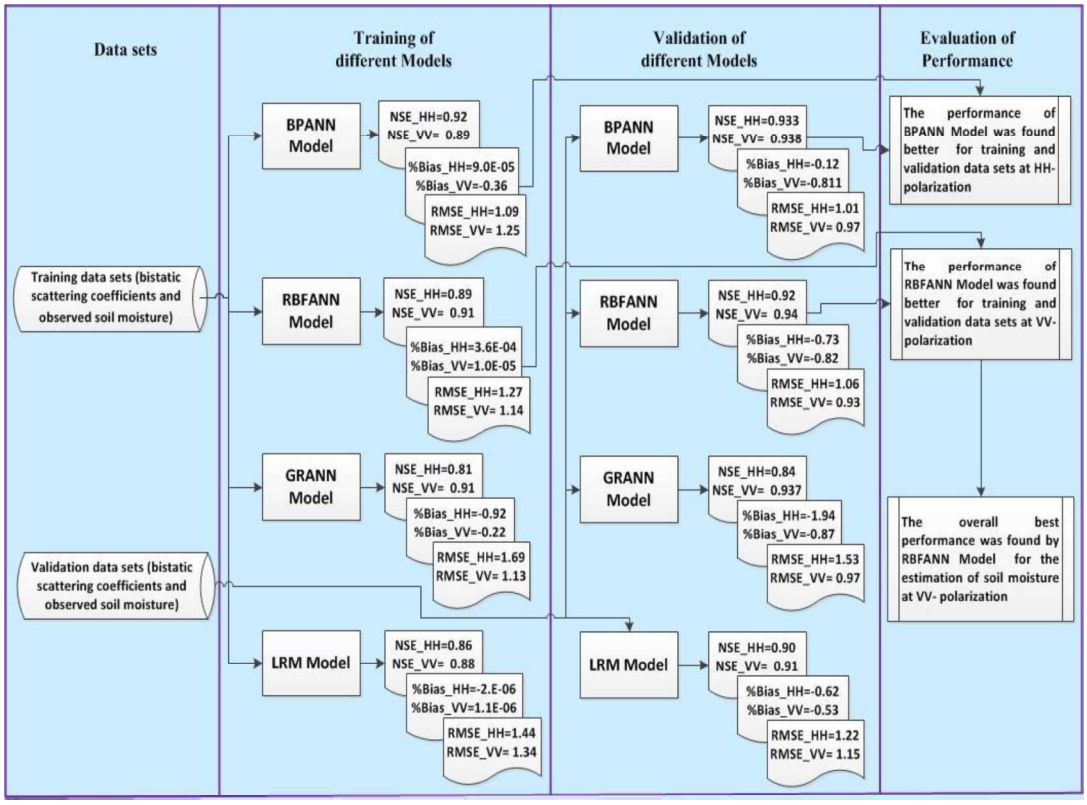

Figure 3.8 Flow chart for the comparison of results

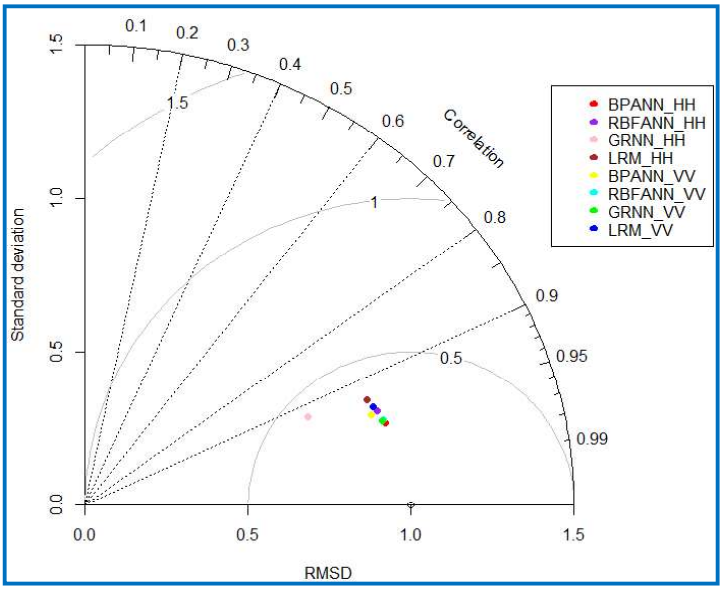

Figure 3.9 Taylor plot for the performance of different models during training at HH- and VV-polarization

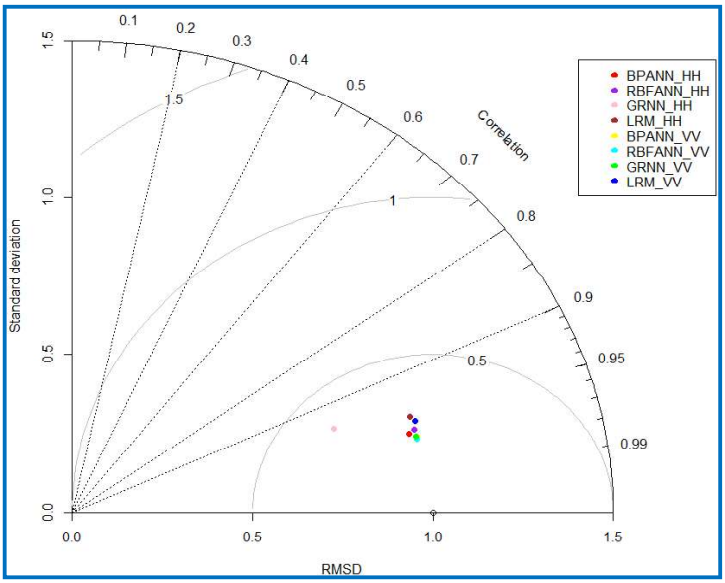

Figure 3.10 Taylor plot for the performance of different models during validation at HH- and VV- polarization

3.6 CONCLUSIONS

The microwave bistatic scattering coefficient was found to increase with the soil moisture content. The dynamic range of bistatic scattering coefficient was found more at VV- polarization than HH- polarization. The suitable incidence angle for the estimation of soil moisture of the slightly rough bare soil surface was found to be 25^0 for both HH- and VV- polarization. All the four models were found suitable for the accurate estimation of soil moisture content using bistatic scatterometer data at HH- and VV- polarizations. However, the performance of these models were found a little better at VV- polarization than HH- polarization for the estimation of soil moisture from slightly rough bare soil surfaces using multi-incidence and dual polarized bistatic scatterometer data. The RBFANN model was found better estimator among the three estimators (BPANN, GRANN and LRM) for the estimation of soil moisture of bare soil surfaces at VV- polarization. The performance of ANN models is found not significantly better than LRM model for the estimation of soil moisture from slightly rough surface using bistatic scatterometer data. Therefore, the LRM model may be the best option than ANN models at VV- polarization. The LRM model is simple than ANN models in operation.